

## <sup>68</sup>Ga-DOTATOC Versus <sup>68</sup>Ga-DOTATATE PET/CT in Functional Imaging of Neuroendocrine Tumors

Thorsten D. Poeppel<sup>1</sup>, Ina Binse<sup>1</sup>, Stephan Petersenn<sup>2</sup>, Harald Lahner<sup>2</sup>, Matthias Schott<sup>3</sup>, Gerald Antoch<sup>4</sup>, Wolfgang Brandau<sup>1</sup>, Andreas Bockisch<sup>1</sup>, and Christian Boy<sup>1</sup>

<sup>1</sup>Department of Nuclear Medicine, University Essen, Essen, Germany; <sup>2</sup>Department of Endocrinology, University Essen, Essen, Germany; <sup>3</sup>Department of Endocrinology, University Dusseldorf, Dusseldorf, Germany; and <sup>4</sup>Department of Diagnostic and Interventional Radiology, University Dusseldorf, Dusseldorf, Germany

Radiolabeled somatostatin analogs represent valuable tools for both in vivo diagnosis and therapy of neuroendocrine tumors (NETs) because of the frequent tumoral overexpression of somatostatin receptors (sst). The 2 compounds most often used in functional imaging with PET are <sup>68</sup>Ga-DOTATATE and <sup>68</sup>Ga-DOTATOC. Both ligands share a quite similar sst binding profile. However, the in vitro affinity of <sup>68</sup>Ga-DOTATATE in binding the sst subtype 2 (sst2) is approximately 10-fold higher than that of <sup>68</sup>Ga-DOTATOC. This difference may affect their efficiency in the detection of NET lesions because it is the sst2 that is predominantly overexpressed in NET. We thus compared the diagnostic value of PET/CT with both radiolabeled somatostatin analogs (<sup>68</sup>Ga-DOTATATE and <sup>68</sup>Ga-DOTATOC) in the same NET patients. **Methods:** Forty patients with metastatic NETs underwent <sup>68</sup>Ga-DOTATOC and <sup>68</sup>Ga-DOTATATE PET/CT as part of the work-up before prospective peptide receptor radionuclide therapy. The performance of both imaging methods was analyzed and compared for the detection of individual lesions per patient and for 8 defined body regions. A region was regarded positive if at least 1 lesion was detected in that region. In addition, radiopeptide uptake in terms of the maximal standardized uptake value (SUVmax) was compared for concordant lesions and renal parenchyma. **Results:** Seventy-eight regions were found positive with <sup>68</sup>Ga-DOTATATE versus 79 regions with <sup>68</sup>Ga-DOTATOC (not significant). Overall, however, significantly fewer lesions were detected with <sup>68</sup>Ga-DOTATATE than with <sup>68</sup>Ga-DOTATOC (254 vs. 262,  $P < 0.05$ ). Mean <sup>68</sup>Ga-DOTATATE SUVmax across all lesions was significantly lower than <sup>68</sup>Ga-DOTATOC ( $16.0 \pm 10.8$  vs.  $20.4 \pm 14.7$ ,  $P < 0.01$ ). Mean SUVmax for renal parenchyma was not significantly different between <sup>68</sup>Ga-DOTATATE and <sup>68</sup>Ga-DOTATOC ( $12.7 \pm 3.0$  vs.  $13.2 \pm 3.3$ ). **Conclusion:** <sup>68</sup>Ga-DOTATOC and <sup>68</sup>Ga-DOTATATE possess a comparable diagnostic accuracy for the detection of NET lesions, with <sup>68</sup>Ga-DOTATOC having a potential advantage. The approximately 10-fold higher affinity for the sst2 of <sup>68</sup>Ga-DOTATATE does not prove to be clinically relevant. Quite unexpectedly, SUVmax of <sup>68</sup>Ga-DOTATOC scans tended to be higher than their <sup>68</sup>Ga-DOTATATE counterparts.

**Key Words:** <sup>68</sup>Ga-DOTATOC PET/CT; <sup>68</sup>Ga-DOTATATE PET/CT; NET

**J Nucl Med 2011; 52:1–7**

DOI: 10.2967/jnumed.111.091165

The abundant expression of somatostatin receptors (sst) is a characteristic of neuroendocrine tumors (NETs). To date, 5 receptor subtypes have been characterized (sst1–sst5) (1,2). NETs typically express several sst subtypes in a pattern related to tumor type, origin, and grade of differentiation (3,4). In most cases, sst2 is overexpressed (3,4). Structural differences between sst subtypes allow for receptor targeting with subtype-specific radiolabeled somatostatin analogs (5). Several analogs are used for peptide receptor radionuclide therapy (PRRT) and scintigraphic imaging or PET of NET. Quite recently, sst PET demonstrated its superiority over scintigraphy and CT (6,7).

The efficiency of a somatostatin analog depends on its specific binding profile. Particularly, the affinity to sst2 is paramount. Two compounds commonly used for sst PET and PRRT are DOTATOC and DOTATATE. Reubi et al. determined the binding profiles of several radiolabeled somatostatin analogs. There were significant differences in subtype-specific affinity after minor structural changes in the radioligand molecule, the introduction of a radiometal, or the use of different radiometals and chelators (2). Yet, the data regarding the analog with the highest uptake in NET shows discrepancies between in vitro and animal data on the one side (2,8,9) and human data on the other (10): Reubi et al. determined the affinity of <sup>68</sup>Ga-DOTATATE in binding sst2 ( $0.2 \pm 0.04$  nM) to be approximately 10-fold higher than that of <sup>68</sup>Ga-DOTATOC ( $2.5 \pm 0.5$  nM) (2). De Jong et al. compared <sup>111</sup>In-diethylenetriaminepentaacetic acid (DTPA)-Tyr3-octreotide and <sup>111</sup>In-DTPA-Tyr3-octreotate (and others) in rats bearing sst-expressing tumors: octreotate exhibited the highest uptake of all compounds tested (8). Storch et al. reported similar results of a comparison including <sup>111</sup>In-DTPA-Tyr0-octreotide and <sup>111</sup>In-DOTA-Tyr3-octreotate (also animal data) (9). However, Forrer et al. could not find relevant differences

Received Apr. 1, 2011; revision accepted Aug. 22, 2011.

For correspondence or reprints contact: Thorsten D. Poeppel, Department of Nuclear Medicine, University Hospital Essen, Hufelandstrasse 55, D-45122 Essen, Germany.

E-mail: Thorsten.Poeppel@uni-due.de

Published online ■■■■■■■■■■

COPYRIGHT © 2011 by the Society of Nuclear Medicine, Inc.

in tumor uptake of  $^{111}\text{In}$ -DOTATOC versus  $^{111}\text{In}$ -DOTATATE in a direct comparison in patients with metastasized NET (10).

The controversy extends into the therapeutic setting, because both compounds are used in PRRT. Because nephrotoxicity is a major concern in PRRT, the dose-limiting factor is often the radiation-absorbed dose to the kidneys (11). Hence, the tumor-to-kidney ratio of a radiopeptide is crucial. The dose is determined by the radiometal and the uptake and retention of the radiopeptide (11–13). Although Forrer et al. reported a higher tumor-to-kidney ratio for  $^{90}\text{Y}$ -DOTATOC than  $^{90}\text{Y}$ -DOTATATE (10), Esser et al. reported results in favor of  $^{177}\text{Lu}$ -DOTATATE versus  $^{177}\text{Lu}$ -DOTATOC (14).

Currently, there is no direct comparison of  $^{68}\text{Ga}$ -DOTATATE and  $^{68}\text{Ga}$ -DOTATOC available regarding tumor uptake and ability to detect NETs. Thus, it is unclear which radiopeptide is preferable for imaging of NET patients.

Therefore, the aim of this study was to compare both the tumor uptake of  $^{68}\text{Ga}$ -DOTATOC with that of  $^{68}\text{Ga}$ -DOTATATE and their diagnostic value in PET/CT in the same patients with metastasized NET.

## MATERIALS AND METHODS

### Patients

Forty patients (27 men, 13 women; mean age  $\pm$  SD,  $56 \pm 19$  y; age range, 27–81 y) were imaged as part of the work-up before prospective PRRT. Imaging is routinely performed with both  $^{68}\text{Ga}$ -DOTATOC and  $^{68}\text{Ga}$ -DOTATATE to determine optimal uptake for treatment with either  $^{90}\text{Y}$ -DOTATOC or  $^{90}\text{Y}$ -DOTATATE. All patients had histologically verified gastroenteropancreatic or bronchopulmonary NETs (plus 1 patient with malignant paraganglioma) and had prior imaging evidence of primary or residual or recurrent disease (primary tumor, metastases, or both). All aspects of patient care and treatment were performed at the discretion of the treating clinicians and according to routine procedures of the department, which are in accordance with the guidelines of the European Neuroendocrine Tumor Society (15). The imaging work-up was performed in accordance with guidelines issued by the university hospital institutional review board. Written informed consent was obtained from all patients. Patients who were treated with somatostatin analogs had received the long-acting formulation. The medication was discontinued before the imaging procedures: the average time of last application was  $5 \pm 1$  wk (range, 3–7 wk; only 3 wk in 1 patient [patient 10], Supplemental Table 1 [supplemental materials are available online only at <http://jnm.snmjournals.org>], because of intense symptoms during withdrawal).

### Radiopharmaceutical Preparation

$^{68}\text{Ga}$  peptides were synthesized in-house according to the method described by Zernosekov et al. (16).  $^{68}\text{Ga}$  was obtained from a  $^{68}\text{Ge}/^{68}\text{Ga}$  radionuclide generator (Eckert & Ziegler). Peptides were obtained from Bachem. Overall preparation time was about 60 min, with a radiochemical yield of 60%–70%. Quality control performed with 2 thin-layer chromatography systems revealed a radiochemical purity of greater than 98%.

### $^{68}\text{Ga}$ -DOTATOC and $^{68}\text{Ga}$ -DOTATATE Imaging

All patients underwent  $^{68}\text{Ga}$ -DOTATOC and  $^{68}\text{Ga}$ -DOTATATE imaging, with an average interval of less than 14 d. Five patients received the  $^{68}\text{Ga}$ -DOTATATE scan initially, and all others received the  $^{68}\text{Ga}$ -DOTATOC scan first.

Imaging was performed using 2 (ECAT) EXACT HR+ PET scanners: one stand-alone system (CTI/Siemens), the other the PET component of an integrated PET/CT scanner (Biograph Emotion Duo; Siemens). Both PET systems had been cross-calibrated. Imaging was performed as previously described (5,17,18). In short, attenuation-corrected whole-body (skull base to upper thighs) scans were acquired in 3-dimensional mode (4-min emission time per bed position, 3-min transmission time on the stand-alone PET, a Fourier-rebinning attenuation-weighted ordered-subset expectation maximization reconstruction algorithm, and smoothing with a 5-mm gaussian kernel). For PET/CT, the CT scan was obtained first using a limited breath-hold technique (CT acquisition parameters for the full- and low-dose protocols: 130 and 15 mAs, respectively; 130 and 110 kV, respectively; slice width, 5 mm; rotation time, 0.8 s; table speed, 8 mm per rotation). Iodinated contrast material was given intravenously using an automated injector. The small bowel was distended by administration of a water-equivalent oral contrast agent (18). To minimize radiation exposure and avoid the repeated use of contrast agents, each patient received only 1 full-dose contrast-enhanced CT scan. Thus, 36 patients received both examinations on the PET/CT scanner (first scan using the full-dose technique and the second scan using the low-dose technique for 32 patients; both scans using the low-dose technique in 4 patients), and 4 patients (with recent external whole-body contrast-enhanced CT) were evaluated on the stand-alone scanner.

### Image Evaluation

Images were initially interpreted visually by 2 experienced nuclear medicine physicians unaware of the results of the other imaging examinations by counting the number of lesions with pathologically increased radiopeptide uptake in the following 8 regions: head and neck, mediastinum, lung, liver, pancreas, abdomen and pelvis (excluding liver and pancreas), bone, and lymph nodes (whole body, i.e., composite of several regions). Only lesions with a morphologic correlate on the CT portion of the full-dose PET/CT scan or on follow-up examinations were considered. Thus, only 31 of the patients with a full-dose PET/CT scan were analyzed in this manner. If more than 5 lesions were visualized within 1 region, the number of lesions was truncated at 5 for that region to avoid bias (19,20). In a second semiquantitative approach, maximal standardized uptake values (SUVmax) were determined in all patients on a lesion-by-lesion basis by 1 of the initial readers. SUV measurements were performed side-by-side on corresponding lesions on fused image datasets. Spheric volumes of interest were drawn closely encircling a lesion, and the SUVmax was obtained. If more than 5 lesions were visualized within 1 organ, only the first 5 lesions in the craniocaudal direction were considered, with the exception of the liver, in which the lesions were traced in the caudocranial direction to avoid attenuation artifacts. Spheric reference volumes of interest were drawn in unaffected liver tissue, the erector spinae muscles, and the gluteal muscles on the left or right side (as appropriate). The native SUVmax of the lesions was normalized to the SUVmax of the liver reference region and to the average SUVmax of the muscle reference regions. A further spheric volume of interest was placed in the renal cortex, avoiding the pelvis and calyces in the left or right kidney (as appropriate).

### Statistical Analysis

Analysis was performed at 3 levels. The first level addressed the aforementioned 8 regions. A region was regarded positive if at least 1 lesion was detected there. The second level analyzed the individual count of lesions per region. At the third level, the

SUVmax of corresponding lesions (overall and in the following 5 subgroups: hepatic metastases, lymphatic metastases, bone metastases, pulmonary metastases, and primary tumor) was compared.

On all levels, results from both groups were also compared with respect to grading (low, intermediate, or high grade) and tumor origin (foregut, midgut, pancreas, or cancer of unknown primary [CUP]). Although pancreatic NETs are foregut in origin, they are regarded here as a separate subgroup because of their somewhat distinct biologic behavior (such as response to therapeutic interventions) and a sufficient sample size.

Nonparametric methods were used. Positive regions were compared using the McNemar test. The number of lesions per region and the SUVmax of corresponding lesions were compared using the Wilcoxon signed-rank test. Scanning parameters were tested for possible differences with the Mann–Whitney *U* test. Potential correlations were tested with Kruskal–Wallis ANOVA or Spearman rank correlation coefficient, as appropriate.

The significance level was 0.05, 2-sided. A Bonferroni adjustment was applied as appropriate. Analyses were performed with STATISTICA (version 8; StatSoft, Inc.).

Moreover, agreement between SUV measurements of both imaging procedures was analyzed on the basis of a Bland–Altman plot (21) of mean differences (Prism 5c; GraphPad Software, Inc.).

## RESULTS

**[Table 1]** Scan parameters and patient characteristics are presented in Supplemental Table 1 and Table 1, respectively. There was no significant difference between both imaging procedures regarding the scanning parameters (uptake time, injected activity, specific activity, and injected peptide mass).

### Regional and Lesional Analyses

Seventy-eight regions (excluding the composite region “lymph nodes”) were found positive with <sup>68</sup>Ga-DOTATATE versus 79 regions with <sup>68</sup>Ga-DOTATOC (Supplemental Table 2). The only discrepant region was head and neck, with 1 positive lymph node in a patient. On average, 3 positive regions were found per patient with each of the imaging procedures. There was no significant difference between either imaging procedure regarding the number of detected regions per patient or the number of patients with at least 1 lesion within 1 of the 8 regions (including the composite region “lymph nodes”) (Supplemental Table 3).

Within the defined regions (excluding the composite region “lymph nodes”), 254 lesions were detected with <sup>68</sup>Ga-DOTATATE versus 262 lesions with <sup>68</sup>Ga-DOTATOC (Supplemental Table 4). The difference was significant (*P* = 0.012). The 8 lesions that were detected additionally with

<sup>68</sup>Ga-DOTATOC were found in 8 patients and were distributed among the following regions: head and neck, lung, liver (3 patients), pancreas, abdomen and pelvis, and bone. On average, 8.2 lesions were found per patient with <sup>68</sup>Ga-DOTATATE versus 8.5 lesions with <sup>68</sup>Ga-DOTATOC. There was no significant difference between either imaging procedure in lesion detection with respect to tumor grading or tumor origin (foregut, midgut, pancreas, or CUP).

### SUV Analyses

Mean <sup>68</sup>Ga-DOTATATE SUVmax across all lesions was 16.0 ± 10.8 versus 20.4 ± 14.7 with <sup>68</sup>Ga-DOTATOC **[Table 2]** (Table 2). The difference was significant (*P* = 0.0005). The difference retained its significance for the normalized values (SUVmax normalized to liver, *P* = 0.012; SUVmax normalized to muscle, *P* = 0.001). The difference retained its significance across the subgroups (hepatic metastases [34 patients], *P* = 0.007; lymphatic metastases [24 patients], *P* = 0.002; bone metastases [17 patients], *P* = 0.008). No significance test was applied to the subgroups primary tumor (11 patients) and pulmonary metastases (5 patients) because of the small sample size.

The mean difference between <sup>68</sup>Ga-DOTATATE and <sup>68</sup>Ga-DOTATOC SUVmax across all lesions was 4.5 ± 9.8 (range, 0.1–55.3). There was no significant relationship between the differences of SUVmax measurements between <sup>68</sup>Ga-DOTATATE and <sup>68</sup>Ga-DOTATOC and tumor grading or tumor origin (foregut, midgut, pancreas, or CUP).

Even though 33 of 40 patients exhibited on average higher <sup>68</sup>Ga-DOTATOC SUVmax than <sup>68</sup>Ga-DOTATATE SUVmax, the tumor uptake varied considerably both within and between patients: 18 patients displayed only lesions with higher uptake of <sup>68</sup>Ga-DOTATOC than <sup>68</sup>Ga-DOTATATE (Fig. 1), 18 patients displayed a mixture of lesions with either higher uptake of <sup>68</sup>Ga-DOTATATE or (predominantly) of <sup>68</sup>Ga-DOTATOC, and 4 patients displayed only lesions with higher uptake of <sup>68</sup>Ga-DOTATATE than <sup>68</sup>Ga-DOTATOC (Fig. 2). **[Fig. 1]** **[Fig. 2]**

There was no significant difference between measurements of SUVmax in patients with or without prior somatostatin analog therapy.

Mean <sup>68</sup>Ga-DOTATATE SUVmax for renal parenchyma was 12.7 ± 3.0 versus 13.2 ± 3.3 with <sup>68</sup>Ga-DOTATOC (Table 2). The difference was not significant for either the native or the normalized values. The tumor-to-kidney ratio was 1.3 ± 0.8 for <sup>68</sup>Ga-DOTATATE and 1.6 ± 1.1 for <sup>68</sup>Ga-

**TABLE 1**  
Scan Parameters

Scan parameter	<sup>68</sup> Ga-DOTATATE			<sup>68</sup> Ga-DOTATOC		
	Mean	SD	Range	Mean	SD	Range
Uptake time (min)	58	32	27–161	68	31	29–162
Activity per dose (MBq)	103	12	60–124	89	16	52–111
Specific activity (MBq/nmol)	50.1	20.8	16.0–95.6	44	22.5	10.9–90.4
Peptide per dose (μg)	6	3	2–13	6	3	2–12

**TABLE 2**  
Tumor Uptake

Group	No. of patients	<sup>68</sup> Ga-DOTATATE						<sup>68</sup> Ga-DOTATOC					
		Native SUVmax		Normalized SUVmax for liver		Normalized SUVmax for muscle		Native SUVmax		Normalized SUVmax for liver		Normalized SUVmax for muscle	
		Mean	SD	Mean	SD	Mean	SD	Mean	SD	Mean	SD	Mean	SD
All	40	16.0	10.8	2.0	2.2	8.6	7.5	20.4	14.7	2.2	1.5	10.3	6.6
Hepatic metastases	34	19.2	11.3	2.4	2.7	10.0	8.6	22.9	12.7	2.5	1.4	11.6	6.4
Bone metastases	17	10.6	8.7	1.4	1.2	6.2	5.1	13.5	12.3	1.7	1.5	7.8	6.3
Lymphatic metastases	24	15.4	9.6	1.8	1.8	8.2	6.7	21.1	16.5	2.2	1.7	10.0	6.7
Pulmonary metastases	5	9.8	5.5	0.8	0.4	4.4	2.5	14.0	8.4	1.1	0.6	5.5	3.0
Primary tumor	11	18.4	12.3	2.5	2.3	11.6	8.5	32.8	22.0	2.7	1.8	14.9	7.5

DOTATOC. The difference was significant ( $P = 0.007$ ). The correlation coefficient of mean SUVmax <sup>68</sup>Ga-DOTATATE and <sup>68</sup>Ga-DOTATOC for renal parenchyma was 0.50 (correlation coefficient SUVmax normalized to liver, 0.59; correlation coefficient SUVmax normalized to muscle, 0.47).

The Bland–Altman plot showed a fair agreement between both measures of sst expression, with a bias toward lower SUVmax measurements in <sup>68</sup>Ga-DOTATATE imaging (Supplemental Fig. 1).

## DISCUSSION

This study demonstrates the high capability of both radiolabeled somatostatin analogs—<sup>68</sup>Ga-DOTATATE and <sup>68</sup>Ga-DOTATOC—to detect lesions from NETs. However, <sup>68</sup>Ga-DOTATOC might be superior to <sup>68</sup>Ga-DOTATATE, presumably because of higher tumor uptake, as indicated by SUVmax. Nonetheless, there was considerable variance in preferential tumor uptake of the 2 compounds.

## Lesion Detection

In our direct comparative study, <sup>68</sup>Ga-DOTATOC was marginally superior to <sup>68</sup>Ga-DOTATATE in detecting NET lesions. The advantage was on the whole and not limited to higher detection rates within one of the evaluated distinct body regions (head and neck, mediastinum, lung, liver, pancreas, abdomen and pelvis, bone, and lymph nodes) or a distinct type of metastatic spread (lymphatic, hepatic, osseous, or pulmonary). Three published studies compared both analogs (coupled to different radiometals) in patients (10,14,22), although mainly for dosimetric purposes. Only Forrer et al. provide some details about lesion detection (10). They investigated the biodistribution and dosimetry of <sup>111</sup>In-DOTATOC and <sup>111</sup>In-DOTATATE in a small set of patients: the results obtained with both compounds were comparable; however, <sup>111</sup>In-DOTATOC enabled better visualization of some liver metastases (10).

Tumor differentiation influences the detection of NET lesions with radiolabeled somatostatin analogs because of a varying capability of expressing sst (23). Moreover, the origin of a NET influences its profile of expression of sst subtypes (24). We examined whether these parameters possessed differential influence on the rate of lesion detection with both tracers. However, we found no significant difference between either imaging procedure in lesion detection with respect to grading (low, intermediate, or high grade) or tumor origin (foregut, midgut, pancreas, or CUP).

## Tumor Uptake

SUVmax of concordant lesions obtained with <sup>68</sup>Ga-DOTATOC was significantly higher than that obtained with <sup>68</sup>Ga-DOTATATE. Normalization either to a tissue with moderate to high sst expression (liver) or to a tissue with low sst expression (muscle) was not able to reduce interpeptide variability and did not cause relevant changes of the results. According to Reubi et al., bronchopulmonary and gastroenteropancreatic NETs are mainly characterized by overexpression of sst1 and sst2 (3,4). Neither <sup>68</sup>Ga-DOTATOC nor <sup>68</sup>Ga-DOTATATE shows relevant binding to sst1 (2). Hence, the higher SUVmax of <sup>68</sup>Ga-DOTATOC is surprising given that <sup>68</sup>Ga-DOTATATE possesses an approxi-

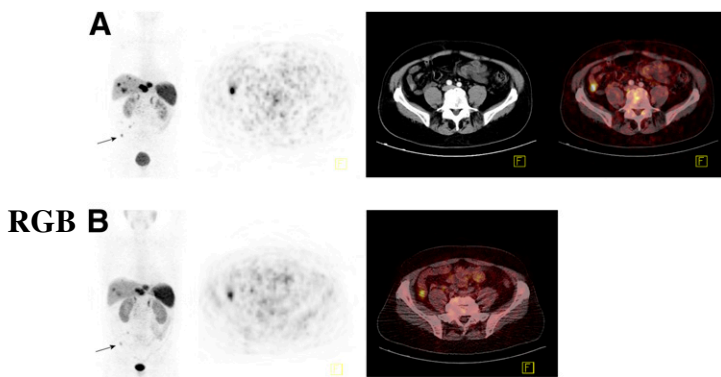


**FIGURE 1.** Example of lesions with exclusively higher uptake of <sup>68</sup>Ga-DOTATOC than <sup>68</sup>Ga-DOTATATE (patient 24). (A, from left to right) <sup>68</sup>Ga-DOTATOC PET maximum-intensity projection, <sup>68</sup>Ga-DOTATOC PET, CT, and PET/CT fusion. (B, from left to right) <sup>68</sup>Ga-DOTATATE PET maximum-intensity projection, <sup>68</sup>Ga-DOTATATE PET, and PET/CT fusion. Arrow refers to ileal carcinoid (SUVmax <sup>68</sup>Ga-DOTATOC, 21.0; SUVmax <sup>68</sup>Ga-DOTATATE, 8.2).

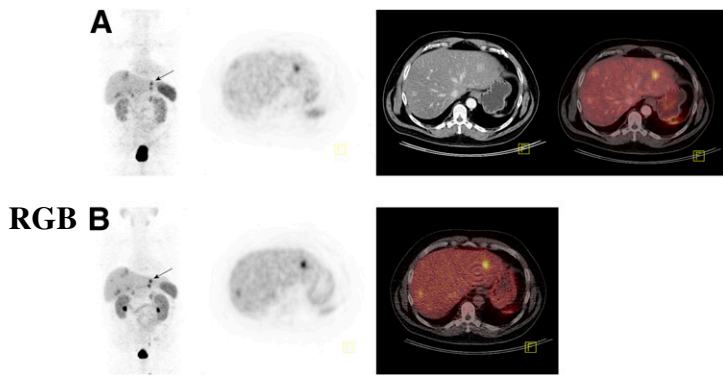


**FIGURE 2.** Example of lesions with exclusively higher uptake of  $^{68}\text{Ga}$ -DOTATATE than  $^{68}\text{Ga}$ -DOTATOC (patient 27). (A, from left to right)  $^{68}\text{Ga}$ -DOTATOC PET maximum-intensity projection,  $^{68}\text{Ga}$ -DOTATOC PET, CT, and PET/CT fusion. (B, from left to right)  $^{68}\text{Ga}$ -DOTATATE PET maximum-intensity projection,  $^{68}\text{Ga}$ -DOTATATE PET, and PET/CT fusion. Arrow refers to hepatic metastasis (SUVmax  $^{68}\text{Ga}$ -DOTATOC, 16.7; SUVmax  $^{68}\text{Ga}$ -DOTATATE, 21.2).

mately 10-fold higher in vitro affinity in binding sst2 ( $0.2 \pm 0.04$  nM vs.  $2.5 \pm 0.5$  nM (2)). However, some NETs exhibit overexpression of sst5 (4,25).  $^{68}\text{Ga}$ -DOTATOC possesses a somewhat increased affinity for this receptor subtype in comparison to  $^{68}\text{Ga}$ -DOTATATE ( $73 \pm 21$  nM vs.  $377 \pm 18$  nM) (2). This difference in affinity profiles might explain the differential tumor uptake. However, this explanation remains hypothetical because no receptor staining of the NET lesions in question was performed.

Our results are in contrast to animal data: De Jong et al. compared  $^{111}\text{In}$ -DTPA-octreotide and  $^{111}\text{In}$ -DTPA-octreotate (and others) both in vitro and in vivo in the same rats bearing somatostatin receptor-expressing pancreatic tumors:  $^{111}\text{In}$ -octreotate possessed the highest uptake in tumors from all compounds tested (8). Storch et al. reported similar results comparing  $^{111}\text{In}$ -DTPA-octreotide and  $^{111}\text{In}$ -DOTA-octreotate (and others) both in vitro and in vivo in rats (9). As mentioned, there are 3 studies comparing biodistribution and dosimetry of both analogs in patients (10,14,22). Forrer et al. found no significant difference in mean residence times and estimated mean absorbed tumor doses for  $^{90}\text{Y}$ -DOTATOC and  $^{90}\text{Y}$ -DOTATATE, although mean doses derived from  $^{111}\text{In}$ -DOTATOC were slightly higher (10). In contrast to these results, Esser et al. reported that  $^{177}\text{Lu}$ -DOTATATE possessed a higher affinity than  $^{177}\text{Lu}$ -DOTATOC in the therapeutic setting. However, data are provided only for residence times (which were longer for  $^{177}\text{Lu}$ -DOTATATE than  $^{177}\text{Lu}$ -DOTATOC). Kwekkeboom et al. also reported higher tumor uptake of  $^{177}\text{Lu}$ -DOTA-octreotate than of  $^{111}\text{In}$ -DTPA-octreotide (22). Yet, they used both a different chelator and a different radiometal in their comparison, which exerts significant influence on receptor binding (2).

The mean difference of all lesional SUVmax measurements between  $^{68}\text{Ga}$ -DOTATATE and  $^{68}\text{Ga}$ -DOTATOC tended to be small; however, there was considerable variance both within and between patients. Nearly half of all patients displayed a mixture of lesions with either higher

uptake of  $^{68}\text{Ga}$ -DOTATATE or (predominantly) of  $^{68}\text{Ga}$ -DOTATOC, most of the remaining patients displayed solely lesions with higher uptake of  $^{68}\text{Ga}$ -DOTATOC, and the minority of patients displayed only lesions with higher uptake of  $^{68}\text{Ga}$ -DOTATATE. Our findings are in line with those of Forrer et al., who found sst expression to vary considerably between patients and tumor manifestations (10). These variations imply the wide spectrum of cellular differentiation and receptor expression of NETs. However, there was no significant relationship between the differences of SUVmax measurements between  $^{68}\text{Ga}$ -DOTATATE and  $^{68}\text{Ga}$ -DOTATOC regarding tumor grading (low, intermediate, or high grade) or tumor origin (foregut, midgut, pancreas, or CUP).

In the case of receptor-active substances, the SUVmax represents a composite measure of specific receptor binding and internalization, unspecific binding, effects of tissue perfusion, and others (26,27). The inpatient comparison approach in this study controls for most confounding factors, rendering differences in SUVmax to be most likely caused by differences in binding and internalization properties of the respective somatostatin analog. However, possible differences in attenuation correction between (predominantly) low-dose PET/CT in  $^{68}\text{Ga}$ -DOTATATE scans and contrast-enhanced PET/CT in  $^{68}\text{Ga}$ -DOTATOC scans may have influenced the results. Yet, those effects seem to be negligible (17,28). In particular, relevant artificial differences are unlikely because the SUVmax of the combination of PET-only scans and low-dose PET/CT for  $^{68}\text{Ga}$ -DOTATOC is still significantly higher than that for its  $^{68}\text{Ga}$ -DOTATATE counterpart ( $P = 0.017$ ). Also, a bias due to slightly longer uptake time of  $^{68}\text{Ga}$ -DOTATOC than  $^{68}\text{Ga}$ -DOTATATE scans cannot be excluded. However, there was no significant difference between the SUVmax of  $^{68}\text{Ga}$ -DOTATATE scans with shorter uptake time and that of scans with longer uptake time than the corresponding  $^{68}\text{Ga}$ -DOTATOC scans. Furthermore, somatostatin analog therapy may affect tumor uptake because of interacting factors such as partial saturation of sst-expressing nontarget tissues and competition of labeled and unlabeled somatostatin analog for the receptor on tumor tissue. On that account, the medication was discontinued before the imaging procedures. Consequently, no significant differences between measurements of SUVmax in patients with or without prior somatostatin analog therapy were found. Because most patients received the  $^{68}\text{Ga}$ -DOTATOC scan as the initial imaging procedure, potential sequence effects cannot be ruled out. These effects may include changes in tumor size or composition between the scans that might have caused a different somatostatin receptor density. However, the mean interscan interval (9 d) was small, compared with typical tumor growth. Relevant changes between the scans thus seem not likely.

#### Renal Uptake

There was no significant difference between renal uptake of either radiopeptide. However, the tumor-to-kidney ratio

found in this study was significantly in favor of  $^{68}\text{Ga}$ -DOTATOC. This finding is in contrast to animal data on  $^{111}\text{In}$ -DTPA-OC and  $^{111}\text{In}$ -DTPA-TATE (9) but is in line with human data derived from a comparison of  $^{111}\text{In}$ -DOTATOC and  $^{111}\text{In}$ -DOTATATE (10). Because nephrotoxicity is a major concern in PRRT (12,13), one might thus speculate about the peptide of preference for therapy to produce optimal tumor doses while avoiding renal impairment (11). However, caution must be taken translating this diagnostic investigation to a therapeutic setting because significantly higher peptide concentrations are used in the latter case. The interplay of unspecific peptide binding, partial saturation of sst-expressing nontarget tissues, and competition of labeled and unlabeled peptide for the receptor on tumor tissue affects overall uptake in the tumor (29,30). Hence, the uptake of radiolabeled somatostatin analogs in sst-expressing tumors is dependent on the amount of injected peptide mass (29). Moreover, not only peptide uptake but also residence times are factors determining the target dose. Esser et al. (14) found the residence times of  $^{177}\text{Lu}$ -DOTATATE to be longer than those of  $^{177}\text{Lu}$ -DOTATOC both in tumors and in kidneys. However, division of the mean tumor residence time ratio by the mean kidney residence time ratio yielded a factor of 1.5 in favor of  $^{177}\text{Lu}$ -DOTATATE. It is thus even more complicated to decide which peptide is to be preferred for radiotherapy. Moreover, tumor uptake shows high inter- and intraindividual variance, with unpredictable preferential of 1 radiopeptide. Only measurements with both radiopeptides reliably permit the choice of the optimal radiopeptide for therapy. Thus, individual dosimetry seems advisable to decide whether a patient can be admitted for therapy with radiolabeled DOTATOC or DOTATATE and to choose the therapeutic modality for each patient.

## CONCLUSION

$^{68}\text{Ga}$ -DOTATOC and  $^{68}\text{Ga}$ -DOTATATE possess a comparable diagnostic value in the detection of lesions of NETs, with a potential advantage for  $^{68}\text{Ga}$ -DOTATOC. The approximately 10-fold higher affinity in binding sst2 of  $^{68}\text{Ga}$ -DOTATATE did not prove to be clinically relevant. Quite unexpectedly, SUVmax measurements with  $^{68}\text{Ga}$ -DOTATOC tended to be higher than their  $^{68}\text{Ga}$ -DOTATATE counterparts.

Nevertheless, there is significant inter- and interindividual variance regarding the radiopeptide with maximal lesional uptake. Thus, our data encourage the application of different sst ligands to permit efficient imaging and therapy of NETs by optimal targeting of tumor receptors.

## REFERENCES

- Hoyer D, Bell GI, Berelowitz M, et al. Classification and nomenclature of somatostatin receptors. *Trends Pharmacol Sci*. 1995;16:86–88.
- Reubi JC, Schar JC, Waser B, et al. Affinity profiles for human somatostatin receptor subtypes SST1-SST5 of somatostatin radiotracers selected for scintigraphy and radiotherapeutic use. *Eur J Nucl Med*. 2000;27:273–282.
- Reubi JC, Waser B, Concomitant expression of several peptide receptors in neuroendocrine tumours: molecular basis for in vivo multireceptor tumour targeting. *Eur J Nucl Med Mol Imaging*. 2003;30:781–793.
- Reubi JC, Waser B, Schaer JC, Laissue JA. Somatostatin receptor sst1-sst5 expression in normal and neoplastic human tissues using receptor autoradiography with subtype-selective ligands. *Eur J Nucl Med*. 2001;28:836–846.
- Boy C, Heusner TA, Poeppel TD, et al.  $^{68}\text{Ga}$ -DOTATOC PET/CT and somatostatin receptor (sst1-sst5) expression in normal human tissue: correlation of sst2 mRNA and SUV(max). *Eur J Nucl Med Mol Imaging*. 2011;38:3–4.
- Buchmann I, Henze M, Engelbrecht S, et al. Comparison of  $^{68}\text{Ga}$ -DOTATOC PET and  $^{111}\text{In}$ -DTPAOC (Octreoscan) SPECT in patients with neuroendocrine tumours. *Eur J Nucl Med Mol Imaging*. 2007;34:1617–1626.
- Gabriel M, Decristoforo C, Kandler D, et al.  $^{68}\text{Ga}$ -DOTA-Tyr3-octreotide PET in neuroendocrine tumors: comparison with somatostatin receptor scintigraphy and CT. *J Nucl Med*. 2007;48:508–518.
- de Jong M, Breeman WA, Bakker WH, et al. Comparison of  $^{111}\text{In}$ -labeled somatostatin analogues for tumor scintigraphy and radionuclide therapy. *Cancer Res*. 1998;58:437–441.
- Storch D, Behe M, Walter MA, et al. Evaluation of [ $^{99m}\text{Tc}$ /EDDA/HYNIC] octreotide derivatives compared with [ $^{111}\text{In}$ -DOTA(0),Tyr3,Thr8]octreotide and [ $^{111}\text{In}$ -DTPA(0)]octreotide: does tumor or pancreas uptake correlate with the rate of internalization? *J Nucl Med*. 2005;46:1561–1569.
- Forrer F, Uusjarvi H, Waldherr C, et al. A comparison of  $^{111}\text{In}$ -DOTATOC and  $^{111}\text{In}$ -DOTATATE: biodistribution and dosimetry in the same patients with metastatic neuroendocrine tumours. *Eur J Nucl Med Mol Imaging*. 2004;31:1257–1262.
- Rolleman EJ, Melis M, Valkema R, Boerman OC, Krenning EP, de Jong M. Kidney protection during peptide receptor radionuclide therapy with somatostatin analogues. *Eur J Nucl Med Mol Imaging*. 2010;37:1018–1031.
- Bodei L, Cremonesi M, Ferrari M, et al. Long-term evaluation of renal toxicity after peptide receptor radionuclide therapy with  $^{90}\text{Y}$ -DOTATOC and  $^{177}\text{Lu}$ -DOTATATE: the role of associated risk factors. *Eur J Nucl Med Mol Imaging*. 2008;35:1847–1856.
- Valkema R, Pauwels SA, Kvols LK, et al. Long-term follow-up of renal function after peptide receptor radiation therapy with  $^{90}\text{Y}$ -DOTA(0),Tyr(3)-octreotide and  $^{177}\text{Lu}$ -DOTA(0),Tyr(3)-octreotate. *J Nucl Med*. 2005;46(suppl 1):83S–91S.
- Esser JP, Krenning EP, Teunissen JJ, et al. Comparison of [ $^{177}\text{Lu}$ -DOTA(0),Tyr(3)]octreotate and [ $^{177}\text{Lu}$ -DOTA(0),Tyr(3)]octreotide: which peptide is preferable for PRRT? *Eur J Nucl Med Mol Imaging*. 2006;33:1346–1351.
- Plöckinger U, Rindi G, Arnold R, et al. Guidelines for the diagnosis and treatment of neuroendocrine gastrointestinal tumours: a consensus statement on behalf of the European Neuroendocrine Tumour Society (ENETS). *Neuroendocrinology*. 2004;80:394–424.
- Zhernosekov KP, Filosofov DV, Baum RP, et al. Processing of generator-produced  $^{68}\text{Ga}$  for medical application. *J Nucl Med*. 2007;48:1741–1748.
- Antoch G, Freudenberg LS, Stattaus J, et al. Whole-body positron emission tomography-CT: optimized CT using oral and IV contrast materials. *AJR*. 2002;179:1555–1560.
- Antoch G, Kuehl H, Kanja J, et al. Dual-modality PET/CT scanning with negative oral contrast agent to avoid artifacts: introduction and evaluation. *Radiology*. 2004;230:879–885.
- Binderup T, Knigge U, Loft A, et al. Functional imaging of neuroendocrine tumors: a head-to-head comparison of somatostatin receptor scintigraphy,  $^{123}\text{I}$ -MIBG scintigraphy, and  $^{18}\text{F}$ -FDG PET. *J Nucl Med*. 2010;51:704–712.
- Therasse P, Arbuck SG, Eisenhauer EA, et al. New guidelines to evaluate the response to treatment in solid tumors. European Organization for Research and Treatment of Cancer, National Cancer Institute of the United States, National Cancer Institute of Canada. *J Natl Cancer Inst*. 2000;92:205–216.
- Bland JM, Altman DG. Statistical methods for assessing agreement between two methods of clinical measurement. *Lancet*. 1986;1:307–310.
- Kwekkeboom DJ, Bakker WH, Kooij PP, et al. [ $^{177}\text{Lu}$ -DOTAOTyr3]octreotate: comparison with [ $^{111}\text{In}$ -DTPA(0)]octreotide in patients. *Eur J Nucl Med*. 2001;28:1319–1325.
- Kayani I, Bomanji JB, Groves A, et al. Functional imaging of neuroendocrine tumors with combined PET/CT using  $^{68}\text{Ga}$ -DOTATATE (DOTA-DPhe1,Tyr3-octreotate) and  $^{18}\text{F}$ -FDG. *Cancer*. 2008;112:2447–2455.
- Koopmans KP, Neels ON, Kema IP, et al. Molecular imaging in neuroendocrine tumors: molecular uptake mechanisms and clinical results. *Crit Rev Oncol Hematol*. 2009;71:199–213.
- Wild D, Macke HR, Waser B, et al.  $^{68}\text{Ga}$ -DOTANOC: a first compound for PET imaging with high affinity for somatostatin receptor subtypes 2 and 5. *Eur J Nucl Med Mol Imaging*. 2005;32:724.

26. Koukouraki S, Strauss LG, Georgoulas V, et al. Evaluation of the pharmacokinetics of  $^{68}\text{Ga}$ -DOTATOC in patients with metastatic neuroendocrine tumours scheduled for  $^{90}\text{Y}$ -DOTATOC therapy. *Eur J Nucl Med Mol Imaging*. 2006;33:460–466.
27. Rodrigues M, Traub-Weidinger T, Li S, Ibi B, Virgolini I. Comparison of  $^{111}\text{In}$ -DOTA-DPhe1-Tyr3-octreotide and  $^{111}\text{In}$ -DOTA-lanreotide scintigraphy and dosimetry in patients with neuroendocrine tumours. *Eur J Nucl Med Mol Imaging*. 2006;33:532–540.
28. Yau YY, Chan WS, Tam YM, et al. Application of intravenous contrast in PET/CT: does it really introduce significant attenuation correction error? *J Nucl Med*. 2005;46:283–291.
29. de Jong M, Breeman WA, Bernard BF, et al. Tumour uptake of the radiolabelled somatostatin analogue [DOTA0, TYR3]octreotide is dependent on the peptide amount. *Eur J Nucl Med*. 1999;26:693–698.
30. Velikyan I, Sundin A, Eriksson B, et al. In vivo binding of [ $^{68}\text{Ga}$ ]-DOTATOC to somatostatin receptors in neuroendocrine tumours—impact of peptide mass. *Nucl Med Biol*. 2010;37:265–275.